EXPERIMENTAL RESULTS OF ANTENNA PLACEMENT TEST ON A CARBON-FIBER SCALE REPLICA OF THE S55X SEAPLANE

R. Fallucca[1], A. Iannuzzo[1], S. Gallina[1], E. Cestino[1] & V. Sapienza[3]

[1]Department of Mechanical and Aerospace Engineering, Politecnico di Torino, 10129 Turin, Italy
[2]Aeronautical Engineering Consultant, Turin, Italy

Abstract

This paper presents the application and the experimental results of a state-of-the-art Antenna Placement testing methodology on a carbon-composite, 1:8 scale replica of the SIAI-Marchetti S55X historical seaplane. As research in the field of drone-based operations is increasing, advanced technologies such as Carbon-Fibre Reinforced Polymers (CFRP) laminates are being implemented in the context of model planes and are thus bringing them to a higher standard of innovation. As a consequence, new challenges arise concerning the aspects of electromagnetic interference and screening effects caused by the conductive carbon-fibre structural elements. This problem is particularly relevant for the S55X scale replica at issue, as it is almost entirely made of CFRP laminates, presents a bulky geometry that easily enables electromagnetic signal interference during most manoeuvres in flight, and therefore needs the peculiar implementation of two, rather than one, onboard receivers. Therefore, designing an ad-hoc Antenna Placement procedure for the S55X replica was key for choosing the optimal positions for the installation of the receivers among those proposed after analysing the manoeuvres allowed in the flight envelope and permitted during an ordinary flight. The test had a significant impact on the optimisation of signal continuity and the reduction of chances of critical failure during all operational phases of flight. The experimental results confirm that the receivers behave best in positions further away from the seaplane's hulls and close to the wing's leading edge, where the interference caused by the signals' reflection on the bulky hulls and wing appear most contained. The present paper can serve as an example of how new challenges with innovative test subjects can be faced by readapting traditional, although state-of-the-art, testing methodologies to push drone-rooted research forward.

Keywords: Antenna Placement, Seaplane, Carbon-Fiber Aircraft, Antenna Pattern

1. The need for Antenna Placement tests on present-day model aircraft

Traditionally, Antenna Placement tests have mostly been conducted on large-scale commercial and military aircraft. The need for such tests in these types of applications is clear and related to the fundamental need for the use of a reliable antenna system during most phases of flight [1]. On the opposite side of the aircraft spectrum, model aircraft falling under the "Open" category of civil drones have rarely, if ever, presented the need to conduct Antenna Placement tests. Their relatively contained bulk, the COTS[1] materials used for their construction (such as processed wood, cloth, styrofoam, EPP, heat-shrink PET, several plastic materials, etc.), and their traditionally imitative geometries have not been causes of failure in the context of transceiver systems. However, as drone-related commerce is expanding worldwide, model aircraft are becoming ever more popular subject matters for several research applications, ranging from electrical hydrogen-fuel-cell-based propulsion to delivery optimisation for humanitarian missions. This renewed interest in model aircraft has pushed for their fast adaptation to advanced technologies such as carbon-fibre-based composite materials, which in fact have been amply used for military aircraft and commercial airliners over the past fifty years.
Following the technological evolution of their large-scale equivalent, present-day model aircraft face the same challenges that military and commercial aircraft faced in the early days of the advent of

[1]Commercial-Off-The-Shelf.

composite materials: Among these appear electromagnetic interference and the optimisation antenna placement, as the risk of signal loss during particular flight manoeuvres poses a safety threat within the entirety of the *Geographical zone*[2] covered by the aircraft. Currently, the most reliable solution to this problem is a full-scale Antenna Placement test that utilises extremely costly and not-so-readily available experimental setups [3]. This paper presents the application of this "traditional", although state-of-the-art, test methodology to a carbon-composite, 1:8 scale replica of the SIAI-Marchetti S55X, which falls under the category of model seaplanes, with the objective to optimise the receiver antennas' placement on the aircraft. This specific application can serve as an example of the types of experimental tests that should, for safety reasons, be conducted on modern, either research- or non-research-oriented, model aircraft that are pioneering the implementation of composite materials in small-scale applications.

2. The S5502: a challenging test article

2.1 Geometry- and material-based issues

The Antenna Placement test described in this paper was conducted on a 1:8 scale replica of the historical catamaran seaplane SIAI-Marchetti S55X, which completed its first flight in 1924 but only earned its international fame in 1933 after completing a transoceanic cruise from Orbetello, Italy, to New York City, USA [4]. With the objective to replicate a long-range, oversea cruise applied in the context of model planes, the SIAI-Marchetti S55X was chosen by the student team "S55" of the Polytechnic University of Turin as the historical aircraft to replicate by implementing modern materials and modern control and propulsion systems, while keeping intact its original design [5], [6].
The S5502 (the 1:8 scale replica at issue, see Fig. 1) maintains its predecessor's peculiar geometry: a 3m wingspan with an aspect ratio of $A.R. = 4.5$, a truss tail supporting a heavy empennage made of a 1m-wide elevator and three rudders, and a catamaran-like hull configuration consisting of two 1.25m-long hulls originally designed to increase the seaplane's stability in water while optimising take-off by reducing drag thanks to their slightly concave profile. This structural arrangement is optimal for heavy take-offs and long-range flights, hence it was almost entirely preserved during the design and realisation phases of the S5502. On the other hand, to increase its structural performance while reducing its overall weight, the student team S55 replaced the original construction materials consisting mostly of wood with a series of composite materials, mostly based on Carbon Fibre Reinforced Polymers (CFRP) laminates [7].

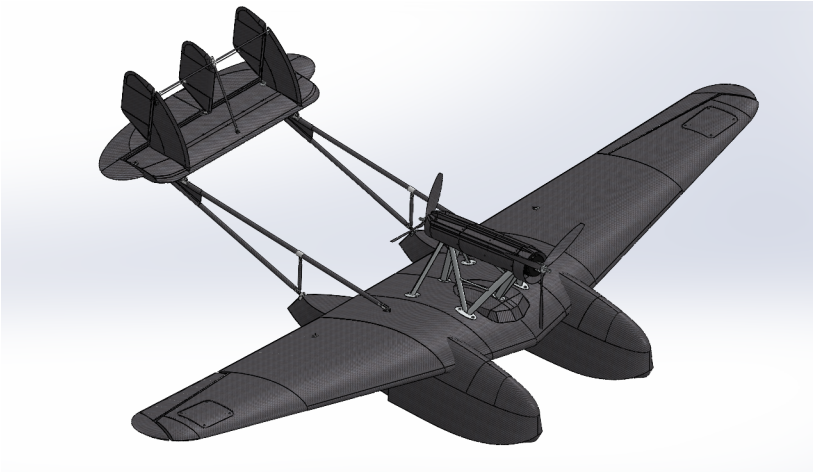

Figure 1 – Test Article: the S5502, a carbon-fibre scale replica of the S55X seaplane

Despite the clear structural advantages derived from the implementation of composite materials in the primary structure of the seaplane, carbon composites pose challenges in the field of electromagnetic interference due to carbon fibre's electrical conductivity, which in turn results in potent interference in transponder applications. The semi-monocoque wing and hulls reflect part of the incoming

[2]Intended as the regulated geographical area where the drone/model aircraft is conducting its mission piloted by a ground operator, who runs safety risks in case of signal loss with its aircraft [2].

electromagnetic signals which then interfere with the received signal in specific flight manoeuvres, increasing the risk of interrupting the continuity of signal reception to the plane from the ground station. This phenomenon is amplified in the context of in-water take-off and splash-down and is thus particularly critical in the case of a remote-controlled model seaplane where live onboard intervention is not permitted. Therefore, in the case of the S5502, it was key to conduct an Antenna Placement test in order to mitigate such risk and prevent critical failures in the context of a VLOS flight with no auto-pilot implemented in the onboard systems.

2.2 Onboard systems and antenna configurations

Although rooted in the tradition of model aircraft, the S5502 can be equated to a *drone* due to the differences between its data management system and that of a common model plane. One of the most crucial aspects of such a data management system is the *transponder system*, which in the case of the S5502 radically differs from that of a traditional model plane in both the number of antennas implemented and their positioning requirements linked to its unusual geometry and electromagnetically problematic construction materials.

As shown in Fig. 2, the S5502's transponder system mainly consists of two *receiver apparati*, also commonly referred to as *receivers*, a communication switch device (from hereon "switch" for simplicity), and a System Flight Controller, which is responsible for the centralised management of all onboard electronics (including the flight controls' servomotors and the propulsion system) and thus also for the processing of the signals coming from the two receivers. Each receiver comprises two monopole antennas held perpendicular to each other and as far away from the aircraft's skin as possible thanks to a fixed motherboard to which they are connected. Such disposition of the monopoles is justified in section 3.1 where the concepts of *signal gain* and *radiation patterns* are introduced.

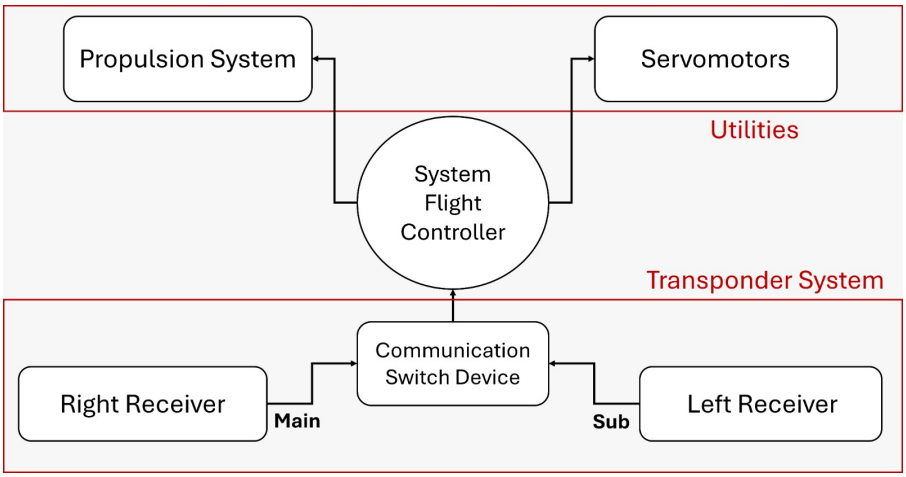

Figure 2 – Transponder system architecture of the S5502

The signal processing occurring within the transponder system follows a precise hierarchy: The two receivers are connected to a switch that prioritises the signal of the "MAIN" receiver over the one coming from the "SUB" (secondary) one. The receiver connected to the "MAIN" port works until it perceives no signal, at which point the receiver connected to the "SUB" port is chosen as the primary receiver. This priority shift is enabled until the "MAIN" receiver reaches acceptable levels of reception again and is now chosen as the leading receiver. De facto, this "MAIN vs. SUB" logic allows for the selection of the strongest signal received by the transponder system at all times as the majority of the manoeuvres planned for flight unavoidably imply the presence of a carbon-fibre structural element (wing, hulls, etc.) invading the leader line between the ground station and one of the receivers. Therefore, implementing two receivers rather than a single one in the transponder system of the S5502 is fundamental to guarantee the continuity of signal reception as it allows for at least one of the two receivers to be always connected to the ground station.

Given the functioning of the transponder system, the objective of the present Antenna Placement test appears clear: locating the two best possible positions for the receivers (one on each half-wing)

among the configurations proposed in subsection 3.2 to ensure reception continuity and, consequently, a safe flight.

3. Antenna Placement testing methodology

3.1 Definition of *signal gain* and *radiation pattern* for a single receiver antenna

Antenna Placement tests are intrinsically based on the concept *signal gain*, which is generally intended as the ratio between the signal intensity compared to the intensity radiated from an isotropic source. A real-life isolated monopole antenna produces an electric field shaped as an almost perfect toroid, i.e. an omnidirectional lobe with cylindrical symmetry about the monopole's axis [8]: It has maximum field intensity on the midplane perpendicular to the antenna, and null on the antenna's axial direction, assuming small deformations of such shape ascribed to crystallographic defects present in the monopole (see Fig. 3).

For the scope of this paper, it is necessary to modify the definition of *signal gain* considering the antenna configuration in the transponder system of the S5502 as described in subsection 2.2 As the receivers are each made of two monopole antennas set perpendicular to each other, the real electric field produced by each receiver has the shape of an almost perfect sphere. Such shape originates from the fact that for each point coordinate around the receiver, the maximum value of the electric field is selected among the fields produced by the single monopole antennas.

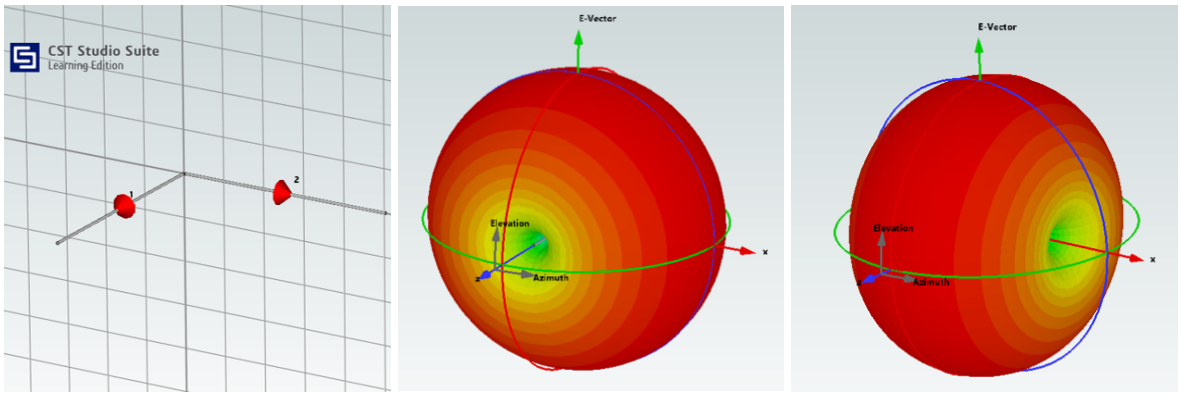

(a) Perpendicular monopoles (b) First monopole (c) Second monopole

Figure 3 – Electric fields produced by monopole antennas set perpendicular to each other.

Although rooted in the concept of transmission, the definition of signal gain can be naturally extended to the context of reception thanks to the symmetry found in an antenna's behaviour in the two working conditions. For this reason, in the present paper, the term signal gain will indicate the subject receiver's ability to *receive*, rather than transmit, an electromagnetic signal compared to an isotropic receiver made of two isotropic monopoles.

The gain of an antenna can be graphically represented through *radiation patterns*, which highlight the distribution of energy transmitted by the antenna from all directions in space; therefore, the most common patterns are either two- or three-dimensional. Unlike an isotropic source, whose three-dimensional radiation pattern returns the image of a perfect sphere, a real receiver placed at a close distance from conductive surfaces (in this case, the S5502's skin) will provide a radiation pattern with different peaks and troughs depending on the interference in a specific direction.

In the case of this investigation, the single measurements of signal gain were obtained from the elaboration of data given by a Vector Network Analyzer (VNA), which is an instrument utilised for measuring and characterising electrical devices working in a specific frequency range and is commonly employed for antenna design and analysis. The instrument records network parameters also known as *scattering parameters* (S-parameters), which for the scope of this study were interpreted to describe how energy is transmitted and/or reflected by the test subject. In the present case, the VNA was connected to a Horn Antenna (often referred to as the *transmitter*, or transmitter antenna, throughout this paper), employed as a signal source, and two monopole antennas simulating only one of the two receivers to be mounted on the S5502 model aircraft. During the test, the VNA provided

values of the signal power P (in dBm)[3] received by each of the two monopole antennas normalised to the power received by an isotropic antenna. The data provided by the VNA was then processed as follows.

$$P[dBm] = 10\log_{10}\left(\frac{P_r[mW]}{1mW}\right)$$
$$P_r[W] = 10^{\frac{P[dBm]-30}{10}} \tag{1}$$

Through conversion Equation 1, power values in Watts were obtained for linear gain calculations. To estimate the signal attenuation at a certain working frequency f and a certain distance ρ, the *Free Space Path Loss (FSPL)* was evaluated, quantifying the power loss of a radio signal with wavelength λ as it propagates in free space from one point (transmitter) to another (receiver) at a distance ρ. In such conditions, it is defined as:

$$FSPL = \left(\frac{\lambda}{4\pi\rho}\right)^2 \tag{2}$$

In the case at hand, the aircraft was placed at a distance $\rho = 2.3m$ (this choice is explained in subsection 3.4), while the wavelength λ was calculated knowing the transmission frequency of the antennas using the well-known formula:

$$\lambda = \frac{c}{f} = \frac{3\cdot 10^8 m/s}{2.4\cdot 10^9 Hz} \approx 0.125m \tag{3}$$

where c is the speed of light in vacuum, and $f = 2.4GHz$ is the transmission frequency. Having calculated the FSPL value, it was possible to obtain the receiving antenna's gain G_r in linear units relative to each data point using the inverse formula of the radio frequency Link Budget, which uses data gathered both during the pre-test and the test itself:

$$G_r = \frac{P_r \cdot FSPL}{P_t \cdot G_t} \tag{4}$$

Equation 4 allowed for the calculation of the power of the signal received by an antenna, given:

- P_r: received power, in Watts (see Equation 1);
- P_t: transmitted power fixed to a value of $3.5\cdot 10^{-4}$ W, set during the pre-test;
- G_t: the gain of the transmitter antenna, in linear units (datasheet value of 10dB);
- FSPL, calculated earlier through Equation 2.

The values of signal gain G_r were then converted from linear to logarithmic units (dB) using Equation 5 and were then used to plot the final radiation patterns presented in section 4.1 to evaluate how varying the receiver's position can affect signal gain.

$$G_r[dB] = 10\log_{10}(G_r) \tag{5}$$

3.2 Receiver positions chosen for the test

Placing the two receivers onboard the S5502 is a fundamental aspect of the model aircraft's design to ensure signal continuity during all operational phases of flight. The objective of this Antenna placement test was to find positions that could present the optimal compromise between the shielding power of the carbon fibres and the requirements imposed by the mission:

[3]The dBm (decibel-milliwatt) is a unit of measurement expressing power relative to one milliwatt (mW); it is widely used in the field of telecommunications to express the power exchange in communication networks or radio transmissions. A 10 dBm increment corresponds to a 10-fold variation in power, which simplifies the analysis of data spanning over several orders of magnitude, as in the case of signal gain measurements.

- At least one of the two receivers must, for the majority of the planned manoeuvres, be connected to the ground station;
- Signal gain must be maximised when possible, also taking into consideration the duration of the single manoeuvres;
- Positioning on structural elements known to cause more intense interference must be avoided;
- Structural elements in contact with water during take-off and splash-down must be avoided.

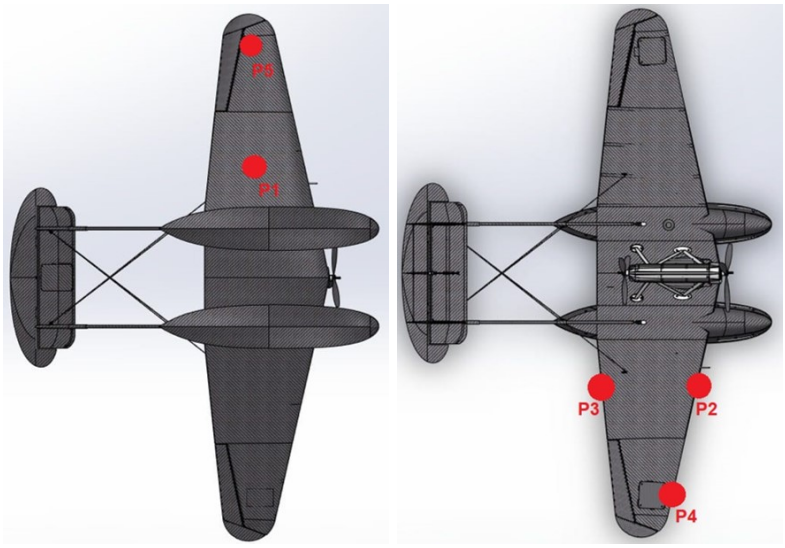

(a) Lower wing surface view (b) Upper wing surface view

Figure 4 – Receiver positions on the lower and upper wing surface of the scale model seaplane

Considering the requirements above, as well as the bulky geometry of the model aircraft, the wing was evaluated as the structural component with the highest number of viable receiver positions. The evaluated positions (presented in Fig. 4) were:

1. Lower surface, circa wing root, mid-chord (**P1**): to cover all manoeuvres with the underside of the wing turned to the ground station (mostly the cruise phase) and not too close to the hulls to avoid interference caused by reflection.
2. Upper surface, circa wing root, leading edge (**P2**): to cover all manoeuvres with the upper side of the wing turned to the ground station (such as take-off and splash-down), not too close to the hulls to avoid interference caused by reflection on the carbon surface, and on the leading edge to ensure better reception continuity during the approach phase.
3. Upper surface, circa wing root, trailing edge (**P3**): to cover all manoeuvres with the upper side of the wing turned the ground station, not too close to the hulls to avoid interference caused by reflection on the carbon surface, and on the trailing edge to ensure better reception continuity during the departure phase.
4. Upper surface, wingtip, leading edge (**P4**): to cover all manoeuvres with the upper side of the wing turned to the ground station, as far away as possible from the hulls to avoid interference caused by reflection on the carbon surface, and on the leading edge to ensure better reception continuity during the approach phase.
5. Lower surface, wingtip, mid-chord (**P5**): to cover all manoeuvres with the underside of the wing turned to the ground station and as far away as possible from the hulls to avoid interference caused by reflection on the carbon surface.

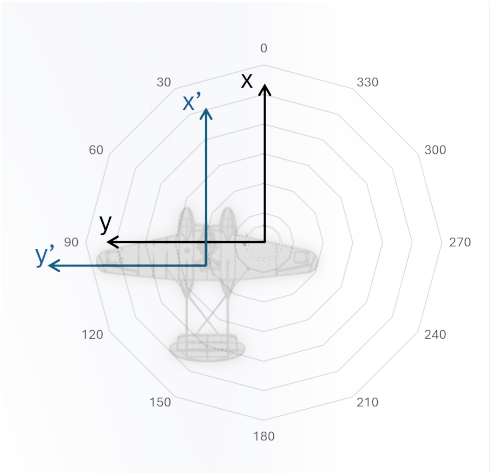

Figure 5 – Reference system alignments as the receiver is moved through positions P_i

Therefore, the objective of the Antenna Placement test presented in this paper was to map the receiver's radiation pattern when moved in each of the five positions P_i, $i = 1,...,5$, and later compare these positions following the steps presented in section 4.2 as a way to choose the best position couple P_iP_j to implement during the installation of the onboard systems on the S5502.

3.3 Coordinate system for radiation pattern mapping

To evaluate the quality of each receiver placement (P1,...,P5), the three-dimensional distribution of signal gain was mapped for each of the above-mentioned five positions by moving the transmitter antenna in discrete points within a polar coordinate system in (ρ, ϕ, θ), with the receiver in its origin as shown in Fig. 6. When moving the receiver through positions P_i, the aircraft's midplane and the wing axis remained parallel to the x-axis and the y-axis of the receiver-centric coordinate system respectively. This can be seen in Fig. 5.
The transmitter had to cover:

- 12 positions in ϕ sweeping $360°$ by $30°$-intervals on the horizontal plane;
- 7 positions in θ ranging from $-90°$ to $+90°$, also swept by $30°$-intervals.

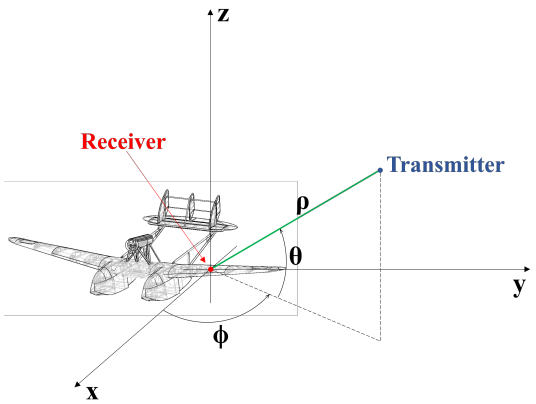

Figure 6 – Polar coordinate system with the receiver at the centre, corresponding in this case to position P2 on the left half-wing. The origin of the coordinate system moves between positions P1 through P5 as radiation patterns are mapped for each one of the receiver positions.

Specifically, as the transmitter is vertically aligned with the receiver when $\theta = \pm 90°$ and thus only one signal gain measurement is possible for all ϕ, the number of discrete transmitter positions in this polar coordinate system amounts to a total of 62 data points for each receiver position. The

transmitter-receiver distance was fixed to the value of $\rho = 2.3m$ throughout the entire measurement campaign.

3.4 Experimental setup

The experimental setup for the test was designed to allow for the mapping of the receiver's radiation patterns as described in subsection 3.3, i.e. covering the 62 discrete positions in the polar reference frame (ρ, ϕ, θ) for each receiver position P_i. Due to the copious amount of data points to collect and consequent setup adjustments to make, the test arrangement was designed to minimise the frequency of human intervention and batch the data-gathering process as much as possible. Hence, instead of having a fixed receiver and a transmitter that should move in (ρ, ϕ, θ), the setup "distributed" the three degrees of freedom among the following elements:

1. **Rotating platform**: responsible for varying ϕ for a fixed ρ and θ. For a correct variation of ϕ, the origin of the polar reference frame described earlier (i.e. the receiver antenna) must lie on the platform's axis of rotation. The floor of the platform was covered with anechoic material to avoid reflection of the transmitter's signal and thus inadvertently affect the receiver's gain.

2. **Support structure**: designed ad-hoc using only dielectric materials (OSB - Oriented Strand Board, MDF - Medium Density Fibreboard, and solid wood) to hold the plane at the height of 1.5m above ground to facilitate manoeuvrability. The structure could support the plane in two different configurations: level flight (Fig. 7a) and inverted flight (Fig. 7b) to allow measurements for all θ despite the transmitter antenna's limitation presented as follows.

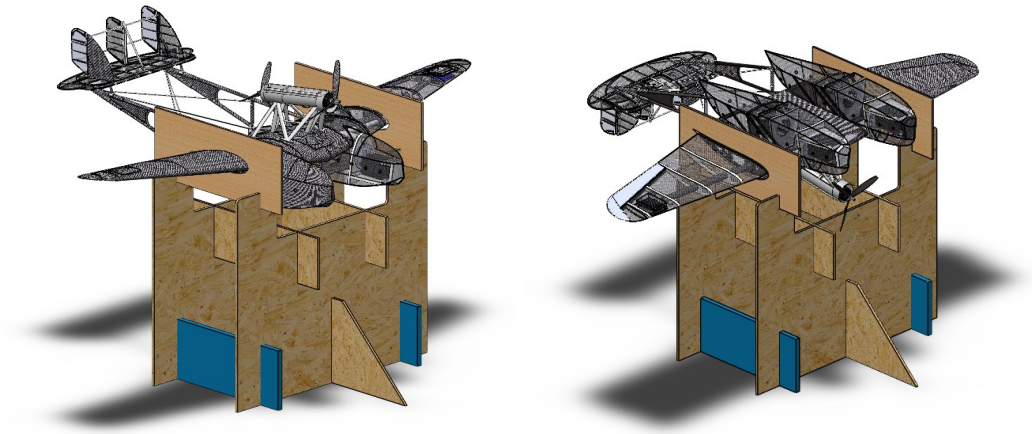

(a) Level flight configuration

(b) Inverted flight configuration

Figure 7 – Possible configurations of the support structure.

3. **Transmitter antenna**: a Horn Antenna mounted on a 9-degrees-of-freedom robotic arm, anchored to the floor outside the rotating platform. The arm was used to control variations in ρ and θ: Once fixed, signal gain data would be collected for all ϕ by rotating the platform by 30°increments. Specifically, the transmitter-receiver distance was kept constant by connecting the two antennas with a 2.3m-long twine while the angle θ between the horizontal plane and the twine, ranging only from 0°to 90°, was measured manually using a construction goniometer and a bubble level. The need to collect data for $\theta \in [-90°, 90°]$ and the range of the transmitter's robotic arm limited to values of $\theta \in [0°, 90°]$ justifies the need to design the support structure to include the inverted flight configuration described earlier as a practical way to cover $\theta \in [-90°, 0°]$.

4. **Receiver antenna**: attached to different structural elements of the plane following positions P_i by using reinforced scotch tape and twine as temporary support to fix it for the time necessary to obtain the 62 data points relative to that specific receiver position. The tape and twine would then be removed and reinstalled for the next iteration of data gathering, relative to the receiver

position P_{i+1}. As the receiver is the origin of the polar reference frame, the plane's relative position to the platform changed for each iteration.

5. **Vector Network Analyzer (VNA) and wiring**: located outside the rotating platform and wired up to the transmitter and the receiver.

Components 1-5 listed above were positioned inside the Anechoic Chamber of *Leonardo S.p.A, Aircraft Division (Caselle Sud plant, Turin, Italy)*, shown in Fig. 8. The facility provided an isolated environment where the Antenna Placement test could be conducted without any external electromagnetic disturbance, helping limit random errors. Due to the significant amount of data points to collect, the test went through one single repetition hence preventing the possibility to make considerations on the single data points' precision and error bar evaluation.

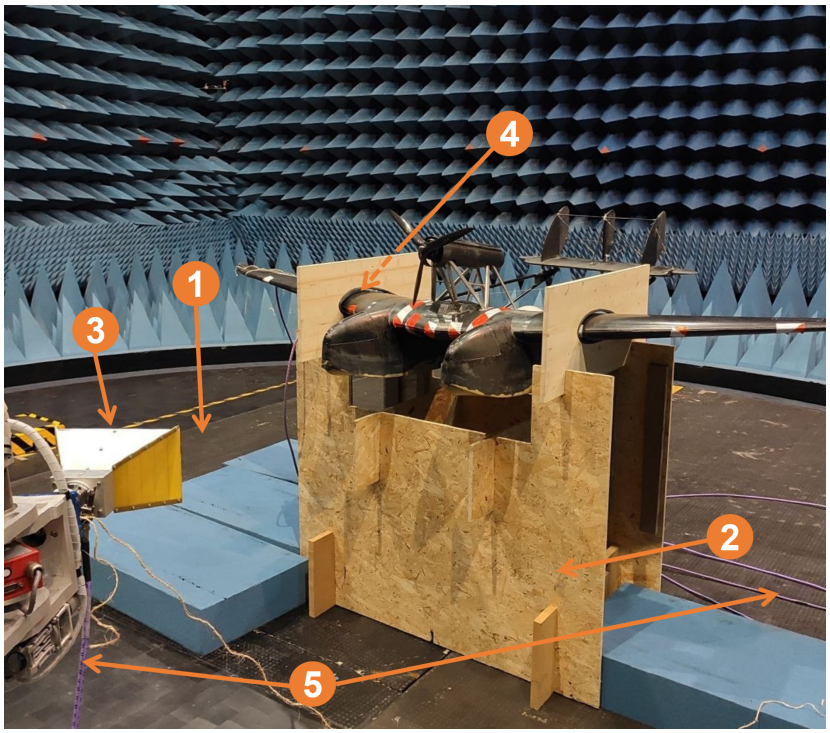

Figure 8 – Test arrangement inside the Anechoic Chamber made available by Leonardo S.p.A for the Antenna Placement test, with labels indicating the setup components listed in subsection 3.4

4. Experimental results

4.1 Individual receiver radiation patterns for positions P_i

Fig. 9 presents the radiation patterns obtained from the processing (following the steps described in subsection 3.1) of raw data collected during the test. The radiation patterns are relative to the receiver, consisting of two monopole antennas, installed in the five positions P_i exclusively on the right half-wing (see subsection 3.2). During the test, the received power values from both monopole antennas were recorded. To determine the final value chosen by the receiver, the highest of the two values was selected in similarity with the functioning of the onboard systems of the S5502 described in subsection 2.2

4.2 Radiation patterns for combinations P_iP_j of receivers

The objective of this investigation was to select the best receiver combination P_iP_j to implement on the S5502 starting from the radiation patterns relative to individual receiver positions P_i, $i = 1,...,5$. The processing of data shown in subsection 4.1 followed the steps listed below:

1. **Radiation patterns for positions P_i mirrored on the left half-wing**
   Considering the aircraft's shape, the radiation patterns of receivers positioned on the left wing

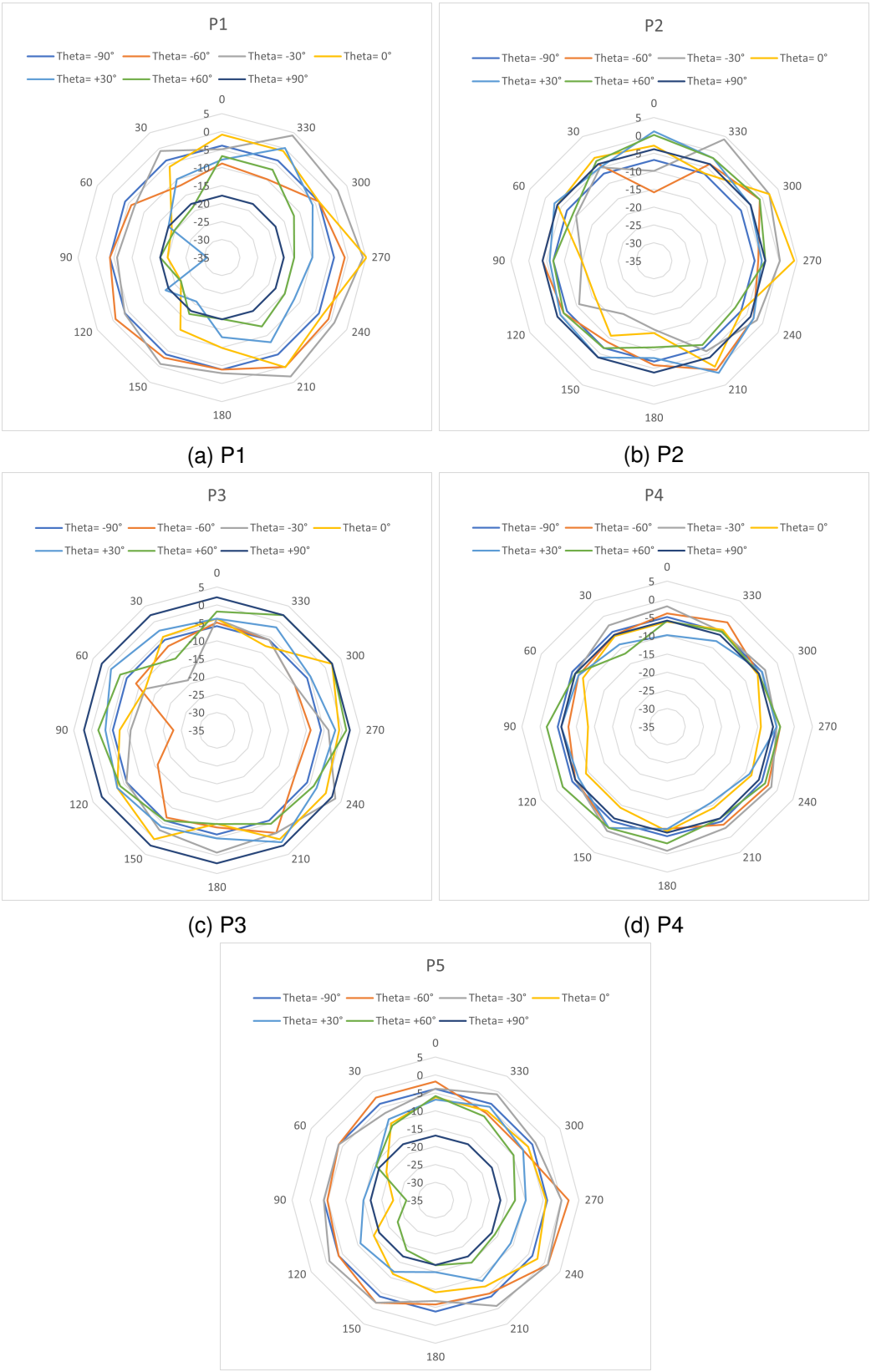

Figure 9 – Radiation patterns of a single receiver antenna in positions P1,...,P5 relative to the right half-wing.

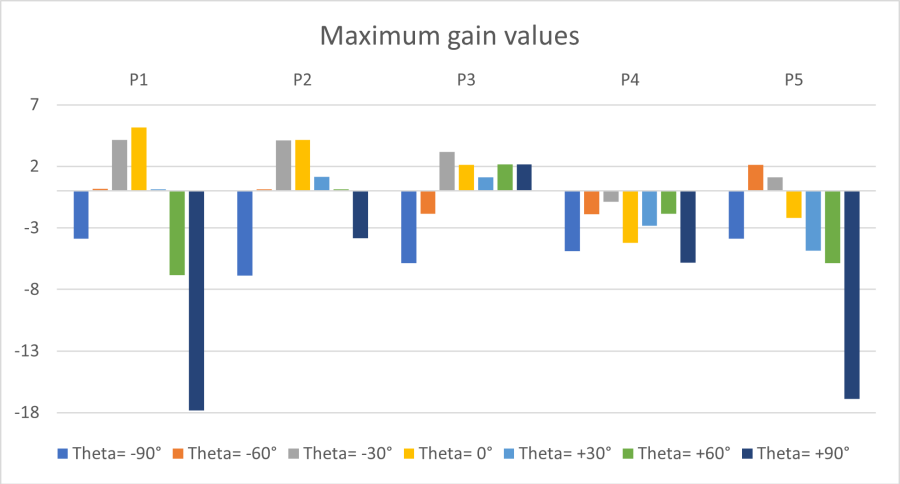

Figure 10 – Maximum gain values for each P_i position.

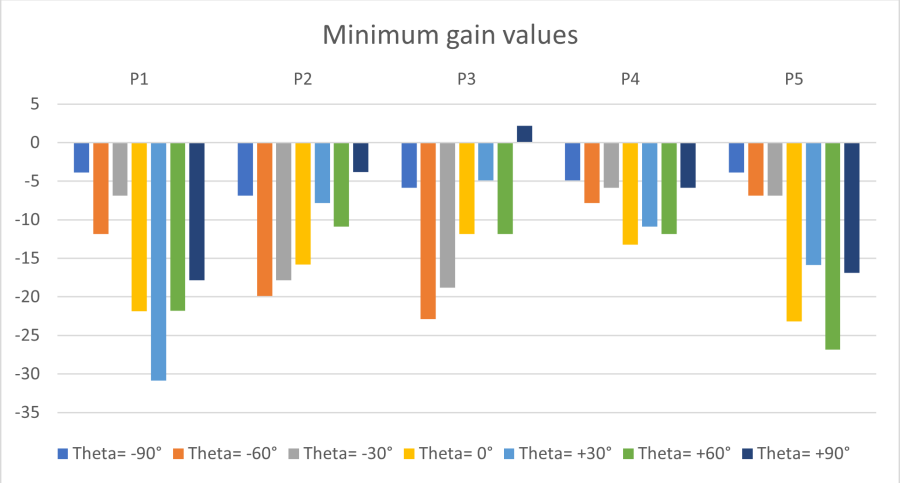

Figure 11 – Minimum gain values for each P_i position.

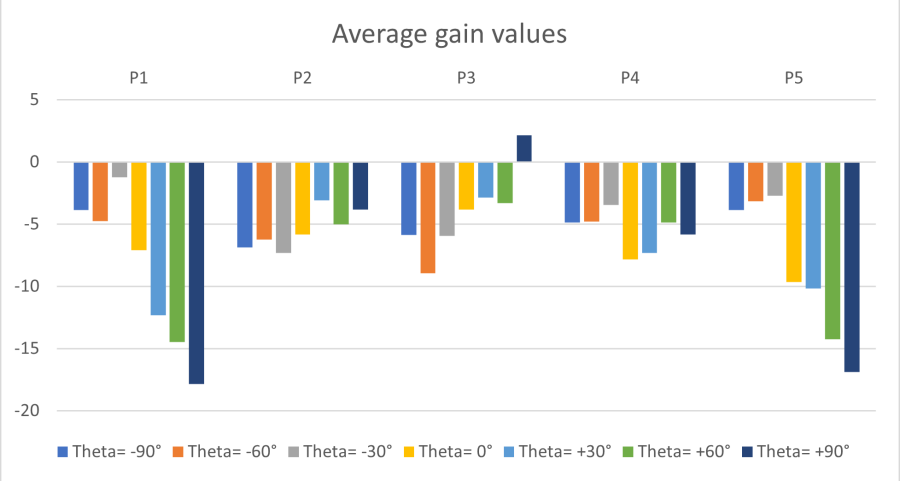

Figure 12 – Average gain values for each P_i position.

were obtained by mirroring the results related to the right half-wing about the aircraft's plane of symmetry.

2. **Exclusion of P_iP_j, $i = j$ receiver couples**

   As stated in paragraph 3.2, the aircraft's reception system must perform effectively during every manoeuvre and minimise the possibility of signal loss in the directions relevant to those manoeuvres. Experimental data show that receivers favouring positive θ values exhibit low gain at negative θ values, and vice versa. Therefore, P_iP_j pairs where $i = j$ have been excluded from the receiver configurations considered and evaluated in section 5.

3. **Definition of P_iP_j radiation patterns**

   The objective of the test is to evaluate the optimal combination of the positions of the two receivers on the S5502 model aircraft, one per half-wing. Therefore, comparisons between symmetrical combinations (e.g. $P_1P_2 = P_2P_1$) have not been made. This approach has also simplified data analysis by reducing the number of radiation patterns to be evaluated. By implementing the *far-field approximation* (see paragraph below), it was possible to obtain the final gain value for each of the P_iP_j combinations by selecting the highest gain value between the two measured in the same (ρ, ϕ, θ) coordinate (see Equation 6), again in imitation of the design of the S5502's transponder system.

$$G_{ij} = \max(G_i, G_j) \tag{6}$$

The resulting graphs are shown in Fig. 13, 14, and 15.

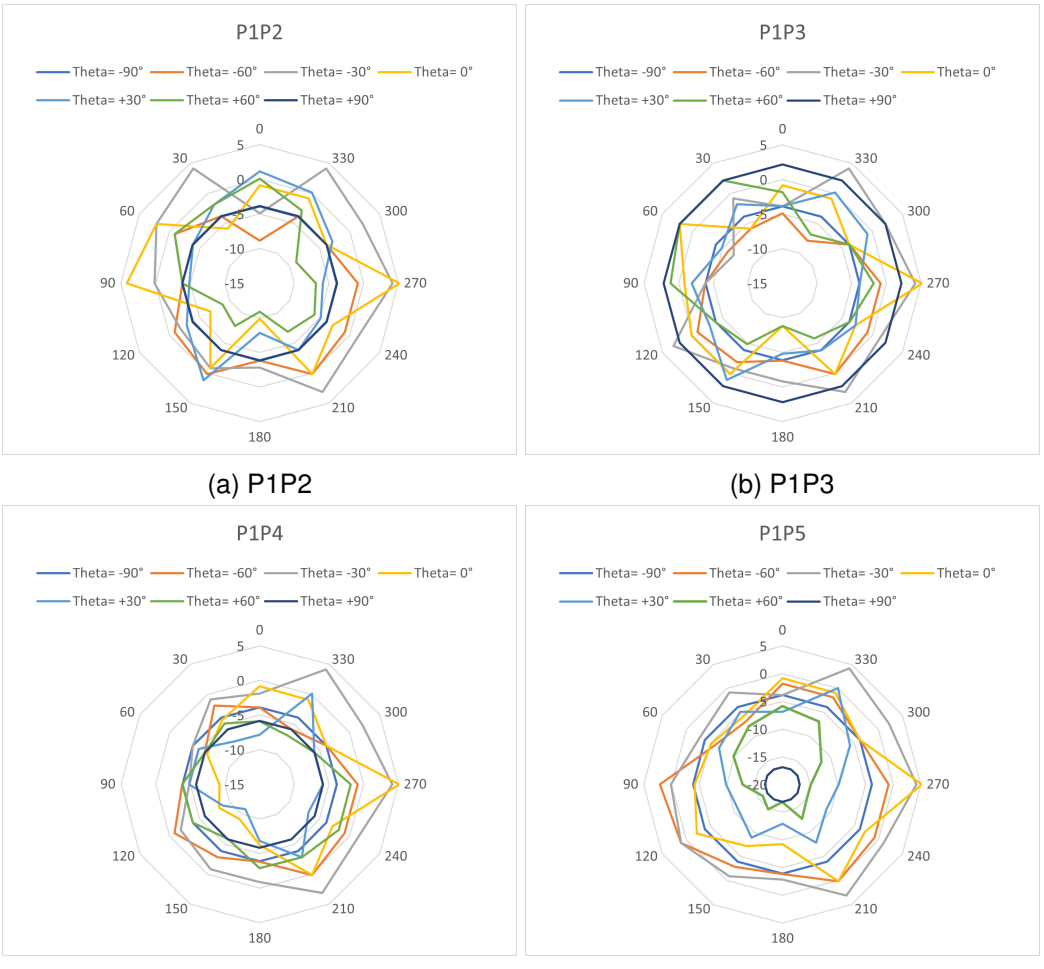

(a) P1P2

(b) P1P3

(c) P1P4

(d) P1P5

Figure 13 – Radiation patterns of receivers in positions P_1P_j, $j = 2, ..., 5$

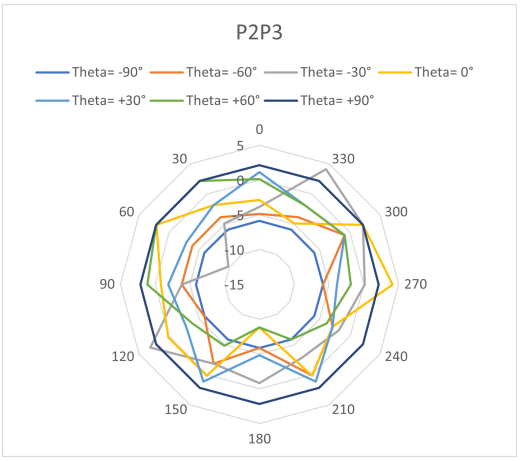

(a) P2P3

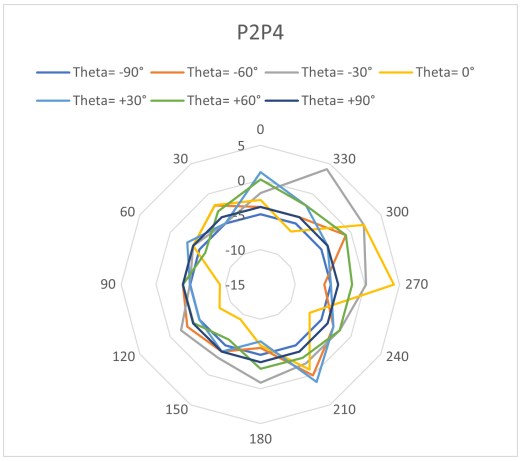

(b) P2P4

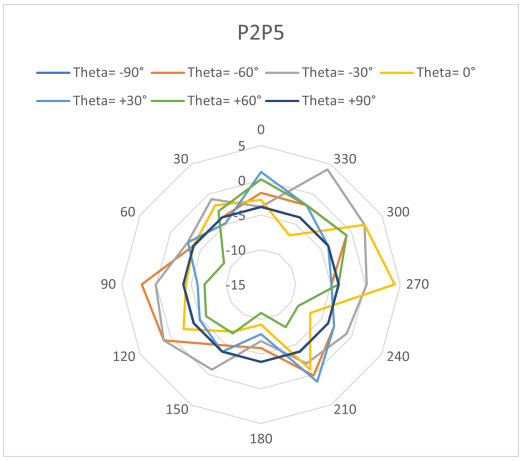

(c) P2P5

Figure 14 – Radiation patterns of receivers in positions P_2P_j, $j = 3, ..., 5$

Far-field approximation This approach allows the source of two electromagnetic signals to be considered point-like at a distance greater than a certain limit distance d calculated using Equation 7. The *far field* of an antenna represents the region of space where electromagnetic waves emitted from a point source "far away" can be approximated as plane waves. This consideration permits the realisation of the radiation patterns for combinations of receivers P_iP_j as if the two were positioned at the same point.

$$d > 10 \cdot \lambda \approx 1.25m \tag{7}$$

As the transmitter was kept at a distance of $\rho = 2.3m > 1.25m$ throughout the test, the far-field approximation is applicable for data analysis.

5. Data Analysis and final P_iP_j placement choice

For the purpose of data analysis, it is important to correlate the different values of θ with the various phases and manoeuvres that must be carried out without losing signal coming from the ground station to preserve the safety of the operators on the ground. Specifically:

- $\theta < 0°$: cruise, turns with the aircraft's underside towards the ground station, descending away from the ground station, ascending approach;
- $\theta > 0°$: turns with the aircraft's upper side towards the ground station, ascending away from the ground station, descending approach;
- $\theta = 0°$: usually occurring during the rapid transition from one flight phase/manoeuvre to another.

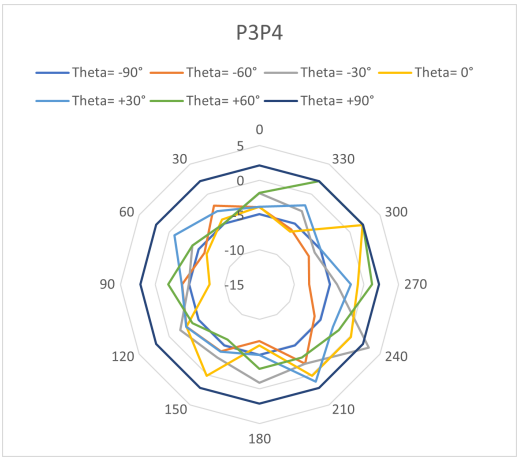

(a) P3P4

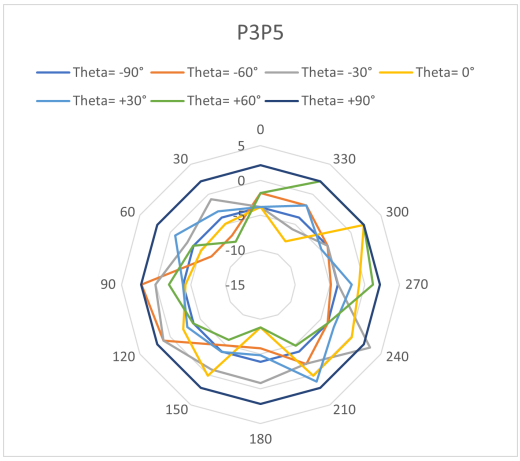

(b) P3P5

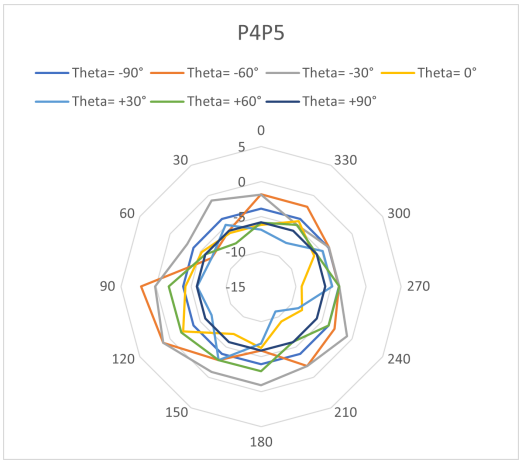

(c) P4P5

Figure 15 – Radiation patterns of receivers in positions P_3P_j, $j = 4,5$ and P_4P_5.

To facilitate data analysis, diagrams of the maximum, minimum, and average gain values were produced for both single positions P_i and for position combinations P_iP_j, as shown in Fig. 16, Fig. 17, and Fig. 18.

5.1 Elimination of receiver combination P_1P_5

Looking at Fig. 16, 17, and 18, it appears clear that the combination P_1P_5 has the worst behaviour compared to all other receiver combinations. As a matter of fact, Fig. 17 shows that P_1P_5 reaches the lowest signal gain value of $G_r = -15dB$ for $\theta = +60°$ and $\theta = +90°$. Furthermore, considering now Fig. 16, the maximum gain value of $G_r = +5dB$ is among the highest maximum registered in the test (combinations P_1P_2, P_1P_3, and P_1P_4 reach it as well) but only for $\theta = 0°$. This behaviour can be justified by making considerations on the receivers' placement: Fig. 4a shows that both P_1 and P_5 are ventral positions, hence all gain values for $\theta > 0°$ are compromised since the carbon-fibre wing is placed between the transmitter and either receiver. This results in powerful dampening when conducting all manoeuvers involving a direct view of the aircraft's top, which is the case of take-off, splash-down, most turns in the initial phases of cruise, and eventually all conditions for which the ground station is located at a higher altitude than the seaplane. As it is key to have the highest possible signal gain values for $\theta \in [60°, 90°]$, the combination P_1P_5 was excluded a priori.

5.2 Elimination of all receiver combinations P_1P_j and P_5P_j

By observing the graphs of the individual receivers (Fig. 9), it is clear that positions P_1 and P_5 have the lowest average gain as θ angle varies. Position P_1 shows, for most of the analyzed angles, quite low and non-uniform gain peaks, which is also observed for position P_5.

From graph 10, it can be noted that the maximum gain values of P_1 are similar to those of the other positions only for angles $\theta = -30°$ and $\theta = 0°$, while for all other angles, the difference in gain reaches as high as $\Delta G_r = 14dB$ specifically in the case of P_1 and P_2 at $\theta = +90°$. Regarding position P_5, for all angles except $\theta = -60°$ and $\theta = -30°$ (where there are maximum values comparable to those of the other positions), the differences in gain reach $\Delta G_r = 12dB$ when considering P_5 and P_2 at $\theta = +90°$.
It is evident that these positions do not contribute significantly to the elaboration of the radiation patterns for pairs P_1P_j and P_5P_j, with $j = 2,3,4$. In fact, graph 10 shows that the maximum gain values of P_1 and P_5 are generally lower than those of the other positions at the same θ angles. In conclusion, by comparing all P_iP_j pairs with each other using graph 18 there appears greater uniformity in signal gain in pairs without positions P_1 and P_5. This allows for the definitive exclusion of all P_1P_j and P_5P_j combinations. The remaining positions to be evaluated in pairs are P_2, P_3, and P_4.

5.3 Remaining combinations and final placement choice

The receiver combinations P_iP_j that exhibited the greatest overall signal gain values are P_2P_3, P_2P_4, and P_3P_4.Comparing Fig. 13, 14, and 15, it can be noticed that these combinations present the best radiation patterns in terms of averages, maximum, and minimum values. To determine the final positioning of the two receivers on the S5502 model plane, it was necessary to evaluate the potential behaviour of the transponder system under specific flight conditions i.e. evaluating the receivers' performance for specific values of θ as specified at the beginning of section 5.
The P_3P_4 combination shown in Fig. 15a presents a rather irregular pattern with minimum peaks of approximately $G_r = -8dB$ for $\theta = -60°$ and $\phi \in [180°, 360°]$. Other gains of similar magnitude were recorded for $\theta = 0°$ and for $\phi \in [0°, 180°]$. In conclusion, P_3P_4 shows above-average gains for $\theta > 0°$, while penalizing $\theta < 0°$, with an overall average gain of approximately $G_{r,avg} = -2.5dB$.
The radiation patterns relative to the P_2P_3 combination shown in Fig. 14a indicate minima of approximately $G_r = -10dB$ for $\theta = -30°, 0°, +60°$. Overall, its radiation pattern is extremely irregular, with elevated peaks followed by highly distanced troughs even in adjacent regions, with such strong variability influencing average gain values. The overall average gain is approximately $G_{r,avg} = -3dB$.
The P_2P_4 combination 14b shows minima of about $G_r = -8dB$ in point coordinates $\theta = 0°$, $\phi \in [90°, 150°]$), maintaining an overall average gain of about $G_{r,avg} = -3.3dB$.
Despite P_2P_4 having slightly lower average gain values compared to the other two options, it also exhibits a more globally regular behaviour, reducing the likelihood that the related measurements were subjected to random experimental errors, preserving a certain level of precision throughout the data collection. Presenting decent gain values for both $\theta < 0°$ and $\theta > 0°$, it is the combination that ensures a globally safer performance for take-off, splash-down, or turning manoeuvres. In conclusion, the P_2P_4 combination was chosen as the best positioning configuration among those proposed earlier in subsection 3.2.

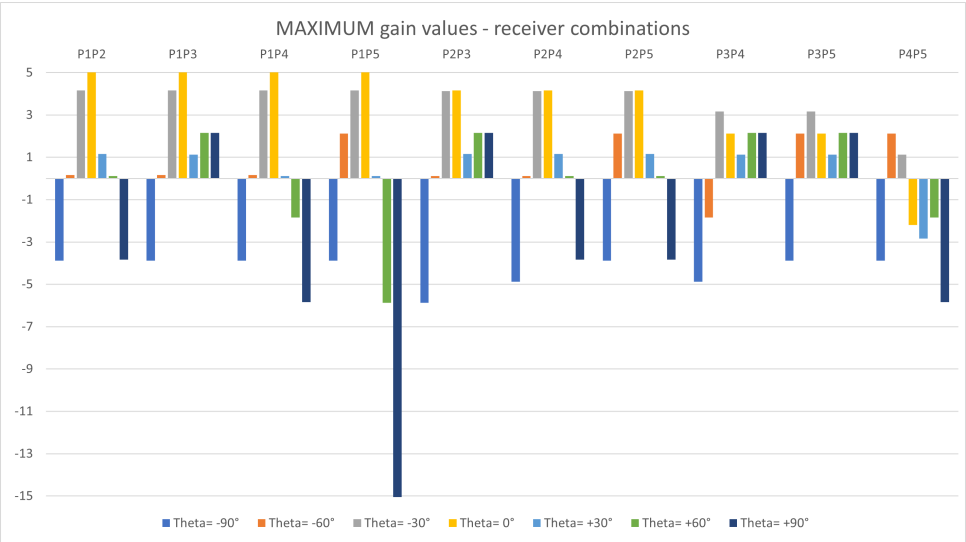

Figure 16 – Maximum gain values for each P_iP_j combination

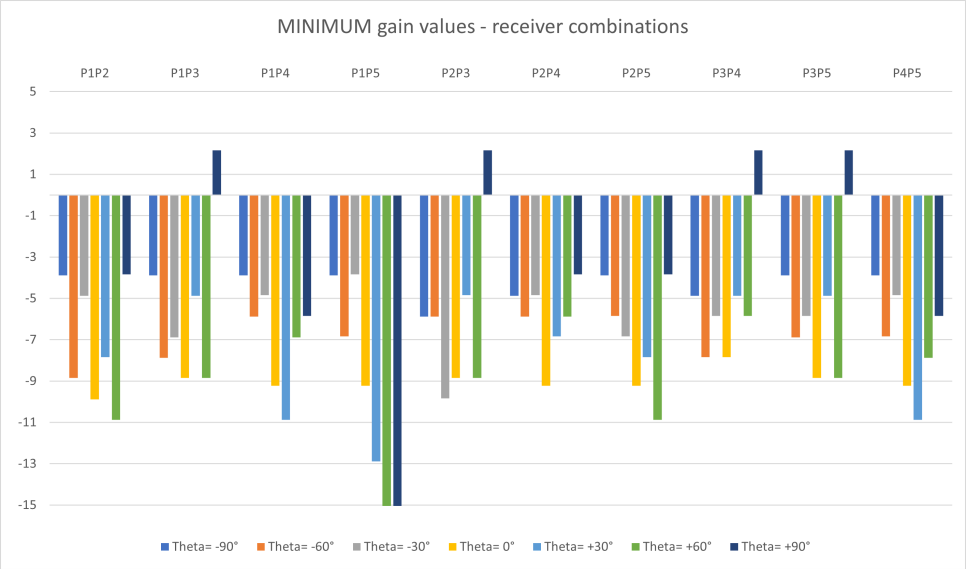

Figure 17 – Minimum gain values for each P_iP_j combination

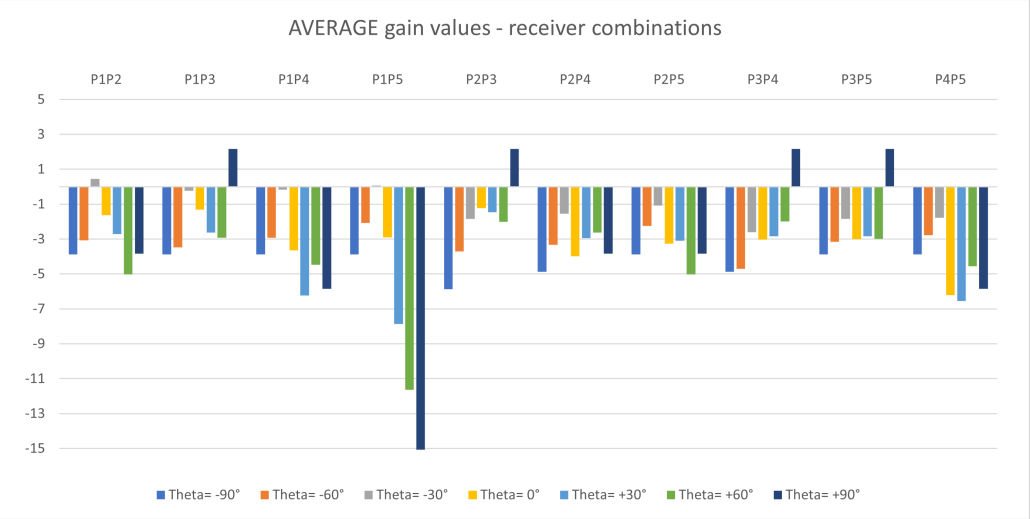

Figure 18 – Average gain values for each P_iP_j combination

6. Conclusions

The analysis conducted in this study has demonstrated how the geometry of a carbon-fibre aircraft influences the radiation patterns of the onboard receivers of its transponder system. The unique properties of carbon fibre, such as high electrical conductivity and electromagnetic shielding capability, are crucial in influencing the behaviour of the receivers. Experimental measurements have shown significant variations in radiation patterns compared to those observed in the case of traditional model aircraft structures.

In a global context where interest in drones continues to grow exponentially, it is essential, even concerning model aircraft, to abandon traditional materials in favour of more advanced and cutting-edge technologies. The experimental results suggest that it is fundamental to approach the design of the transponder system of a carbon-fibre aircraft by taking into account the positioning of the receivers as an important variable to be optimised. This approach should consider not only the material properties but also the overall geometry of the aircraft. Failure to consider these effects can severely compromise the effectiveness of onboard communication and navigation systems.

Antenna Placement tests enable to benefit from the properties of these materials reducing their negative impact on signal reception. Additionally, these tests can facilitate technological advancement

and optimise communication and control performance, offering more precise and efficient solutions for signal management in all operational conditions.
In conclusion, a thorough understanding of the interactions between the geometry of a carbon-fibre aircraft and the radiation patterns of its receivers is crucial for improving the reliability and efficiency of onboard communication systems. The results of this study provide a significant contribution to model aircraft telecommunication design, paving the way for further research and technological developments in this field.

7. Copyright Statement

8. Contact information

For further information, please contact:
Enrico Cestino - enrico.cestino@polito.it
Rosy Fallucca - rosyfallucca4@gmail.com

9. Acknowledgments

The authors would like to thank Leonardo S.p.A., Aircraft Division, for establishing a fruitful partnership with Student Team S55 from Polytechnic University of Turin, Italy. Such collaboration led to the complete realisation of the Antenna Placement test presented in this paper, which includes the incredible opportunity to use Leonardo S.p.A's anechoic chamber facility for the test, as well as the mentoring and assistance given to Team S55 throughout the whole process.

References

[1] Frid H. "Analysis and Optimization of Instaled Antenna Performance." Ph.D. thesis, KTH Royal Institute of Technology, Stockholm, Sweden, 2020.

[2] "Geo-Zones – know where to fly your drone." European Union Aviation Safety Agency. https://www.easa.europa.eu/en/light/topics/geo-zones-know-where-fly-your-drone (accessed May 24, 2024)

[3] Lewis D.M., Bommer J., Hindman G.E. and Gregson S.F. "Traditional to Modern Antenna Test Environments: The Impact of Robotics And Computational Electromagnetic Simulation on Modern Antenna Measurements." *15th European Conference on Antennas and Propagation (EuCAP)*, Dusseldorf, Germany, 2021.

[4] Cestino E., Frulla G., Sapienza V., Pinto P., Rizzi F., Zaramella F. and Banfi D. "Replica S55 Project: a wood seaplane in the era of composite materials." *31st Congress of the International Council of the Aeronautical Sciences*, Belo Horizonte, Brazil, 2018.

[5] Loiodice L., Brugnera A., Di Cosmo D., Di Domenico V., Fallucca R., Grendene S., Piani R. and Prodan M. "Design and building a 1:8 scale replica of the SIAI Marchetti S55X." *Italian Association of Aeronautics and Astronautics, XXVI International Congress,* Pisa, Italy, 2021.

[6] Di Ianni L., Loiodice L., Celestini D., Tiberti D., BaldonC., Iavecchia P., Saponaro Piacente A., Prodan M., Grendene S., Barberis B. and Santoro L. "Team S55: 1:8 scale "replica" of the SIAI-Marchetti S55X." *33rd Congress of the International Council of the Aeronautical Sciences*, Stockholm, Sweden, 2022.

[7] Loiodice L., Grendene S., Binetti T., Boni I., Lovero F. and Piani R. "Study of the cost efficiency and laminate quality using different mould-making technologies." *33rd Congress of the International Council of the Aeronautical Sciences*, Stockholm, Sweden, 2022.

[8] Balanis C.A. *Antenna Theory: Analysis and Design*. 3rd edition, John Wiley & Sons, Inc., 2005.